Division of Nuclear Charge Deduced from X-Ray Measurements in the Spontaneous Fission of ^{252}Cf†

L. E. GLENDENIN AND J. P. UNIK
Argonne National Laboratory, Argonne, Illinois
(Received 21 July 1965)

The variation of nuclear charge with mass in the spontaneous fission of ^{252}Cf has been investigated by simultaneous measurement of the masses and characteristic K x-ray energies associated with the fission fragments. The K x rays were detected by a thin NaI(Tl) scintillator or by an argon-filled proportional counter in coincidence with a pair of solid-state detectors for the complementary fission fragments. The yield and energy of K x rays emitted in the first centimeter ($\sim$1 nsec) of fragment flight were determined as a function of fragment mass. The yield of K x rays per fragment is a pronounced function of mass, rising from 0.04 in the region of mass (after neutron emission) below 98 ($N<59$) to a maximum of 0.13 near the center of the light group, falling to 0.05 in the mass region 131-135 ($Z\approx50$, $N\approx82$), rising to 0.15 near the center of the heavy group, and then increasing rapidly beyond mass 145 (region of deformed nuclei) to a peak of 1.0 around mass 154. The observed correlation of K x-ray energies with fragment mass leads to a most probable nuclear-charge (Z_P) function in better agreement with the empirical rule of equal charge displacement (ECD) than with other postulates for charge division in nuclear fission.

I. INTRODUCTION

SINCE the earliest studies[1] of the distribution of nuclear charge in fission by the indirect radiochemical method of fractional chain-yield measurements, the desirability of a more direct physical approach to the problem has been recognized. The results of one such approach have been reported by Armbruster *et al.*[2] Their method involves primarily the measurement of the average β-decay-chain length as a function of mass by absolute counting of the β particles emitted by mass-separated fission products. These results (for thermal-neutron-induced fission of U^{235}) are in disagreement with the charge division deduced from the large body of radiochemical data obtained over the past 20 years and recently summarized by Wahl *et al.*[3]

With the discovery of the emission of characteristic fission-fragment x rays coincident with fission[4–7] it became obvious that a direct physical determination of the most probable nuclear charge (Z_P) of fission fragments as a function of mass (A) is attainable from simultaneous measurements of the characteristic x-ray energies and complementary fragment masses associated with a fission event. The recent development of solid-state detectors with good mass resolution for fission fragments [full width at half maximum (FWHM)$\approx$4 amu for fission of ^{252}Cf] has made this method most attractive.

Preliminary to this three-parameter study of charge division, the gross characteristics of the K x rays were examined in some detail and reported previously.[8,9] The total yield of K x rays was found to be 0.57$\pm$0.06 per fission, the light and heavy groups accounting for 0.17$\pm$0.02 and 0.40$\pm$0.04, respectively. From delayed-coincidence and fragment time-of-flight experiments it was found that about 30% of the K x rays are emitted within 0.1 nsec after fission, another 30% between 0.1 and 1 nsec, 25% between 1 and 10 nsec, the remaining 15% appearing as two delayed components of equal intensity with half-lives of $\sim$30 and $\sim$100 nsec. These characteristics are consistent with the formation of the K x rays by the relatively slow process of internal conversion during de-excitation of the fission fragments rather than by the much faster process of K x-ray emission ($\sim10^{-16}$ sec) that would result from any K vacancies caused by a disruption of the electron cloud directly in the act of fission.

In this paper are reported the final results of an investigation of charge division (Z_P versus A) in the spontaneous fission of ^{252}Cf presented earlier in preliminary form.[9,10] The procedure consists of a three-parameter measurement of the K x rays in coincidence with complementary fission fragments whose kinetic energies are determined with a pair of solid-state detectors. The measured K x-ray energies define the

† Based on work performed under the auspices of the U. S. Atomic Energy Commission.

[1] L. E. Glendenin, C. D. Coryell, and R. R. Edwards, *Radiochemical Studies: The Fission Products*, edited by C. D. Coryell and N. Sugarman (McGraw-Hill Book Company, Inc., New York, 1951); National Nuclear Energy Series, Plutonium Project Report, Vol. 9, Div. IV, p. 489 (unpublished).

[2] P. Armbruster, D. Hovestadt, H. Meister, and H. J. Specht, Nucl. Phys. **54**, 586 (1964).

[3] A. C. Wahl, R. L. Ferguson, D. R. Nethaway, D. E. Troutner, and K. Wolfsberg, Phys. Rev. **126**, 1112 (1962).

[4] V. K. Voitovetskii, B. A. Levin, and E. V. Marchenko, Zh. Eksperim. i Teor. Fiz. **32**, 263 (1957) [English transl.: Soviet Phys.—JETP **5**, 184 (1957)].

[5] V. V. Sklyarevskii, D. E. Fomenko, and E. P. Stepanov, Zh. Eksperim. i Teor. Fiz. **32**, 256 (1957) [English transl.: Soviet Phys.—JETP **5**, 220 (1957)].

[6] R. B. Leachman, *Proceedings of the International Conference on the Peaceful Uses of Atomic Energy, Geneva, 1958* (United Nations, Geneva, 1958), Vol. 15, p. 331.

[7] V. V. Sklyarevskii, E. P. Stepanov, and B. A. Medvedev, Zh. Eksperim. i Teor. Fiz. **36**, 326 (1959) [English transl.: Soviet Phys.—JETP **9**, 225 (1959)].

[8] L. E. Glendenin and H. C. Griffin, Phys. Letters **15**, 153 (1965).

[9] L. E. Glendenin, J. P. Unik, and H. C. Griffin, Proceedings of the IAEA Symposium on the Physics and Chemistry of Fission, Salzburg, 1965, paper SM-60/31 (to be published).

[10] J. P. Unik and L. E. Glendenin, Bull. Am. Phys. Soc. **10**, 13 (1965).

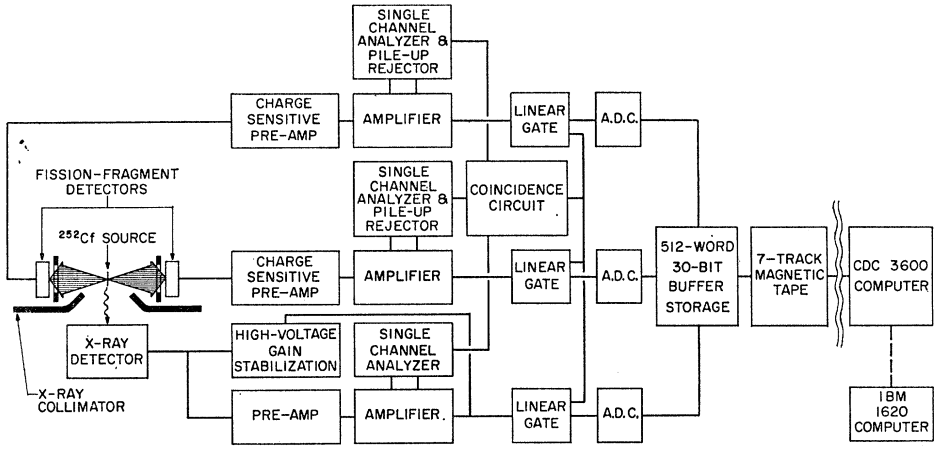

FIG. 1. Schematic diagram of source and detector arrangement and data recording system used in the three-parameter investigation of nuclear charge division in spontaneous fission of ^{252}Cf.

nuclear charges (or atomic numbers), and the masses of the fragments are calculated from the observed kinetic energies. The availability of ^{252}Cf for the first investigation by this method proved to be of great value since a spontaneously fissioning source facilitates probing of the various aspects of the experimental method and obviates the difficulties often associated with the use of a reactor or an accelerator. A further advantage, undoubtedly owing to this great convenience, is that a wealth of detailed information (obtained with high-resolution time-of-flight techniques) is now available on the characteristics of ^{252}Cf fission such as mass distributions, neutron emission and total kinetic energy as a function of mass, and other data required for accurate determination of fragment masses with solid-state detectors.

II. EXPERIMENTAL

A. Procedure and Apparatus

Essentially weightless sources of ^{252}Cf for this investigation were prepared by volatilization in vacuum from a hot filament onto a thin carbon film ($\sim$30 μg/cm^2) which was then placed between two supporting films of VYNS plastic (each $\sim$15 μg/cm^2) on a source holder. The intensity of the source used in two experiments with NaI(Tl) as the x-ray detector (100 nsec coincidence resolving time) was $\sim$4000 fissions/sec (f/sec); a source of less intensity ($\sim$1600 f/sec) was required in two experiments using a gas-flow proportional x-ray detector (2 μsec coincidence resolving time) in order to achieve a reasonably low ratio ($\sim$10%) of chance to true coincidence rates.

A schematic diagram of the arrangement of the source and detectors, the electronic system, and the data recording and computing equipment is shown in Fig. 1. The ^{252}Cf source was located between two fission-fragment detectors at a distance of 2 cm from each. The detectors (n-type surface-barrier) were operated at an optimum bias (60–70 V) for minimum change in response with the increasing leakage current due to damage by fission fragments. A circular "doughnut-shaped" aluminum collimator on each fission detector defined a detection area of 2.0 cm^2 (geometric efficiency $\sim$5%). A copper collimator (0.75 g/cm^2) was placed so as to restrict the "view" of the x-ray detector to x rays originating from fission fragments in the first cm ($\sim$1 nsec) of flight, corresponding to about 60% of the total K x-ray emission. This collimation served not only to maintain a reasonably well defined geometric efficiency for x-ray detection but, more importantly, to avoid measurement of K x rays from delayed transitions (>1 nsec) in the fragments which might emphasize a particular nuclear charge rather than the average for a given mass region. The fission source, detectors, and x-ray collimator were enclosed in an aluminum vacuum chamber (maintained at a pressure of $\sim$10 μ) equipped with a beryllium window (282 mg/cm^2) for high x-ray transmission.

The x-ray detector (with a 95 mg/cm^2 Be window) was located outside the chamber at 90° to the flight path of the fragments (for minimum Doppler broadening) at a distance of $\sim$4 cm from the ^{252}Cf source (geometric efficiency $\sim$3%). Two types of x-ray detectors were used: a NaI(Tl) scintillator (25 mm diam $\times$3 mm thick) and a gas-flow (90% argon-10% methane) proportional counter (9 cm diam) operated at atmospheric pressure. A gain stabilization circuit which sensed the peak amplitude for an x-ray monitor (Fe^{55}) and controlled the high-voltage supply to the proportional counter was used to counteract gain drift caused by variations in atmospheric pressure. The absolute counting efficiencies and energy response functions for x rays measured with these detectors in each experiment were determined with standardized samples of ^{55}Fe, ^{65}Zn, ^{85}Sr, ^{109}Cd, ^{137}Cs, ^{141}Ce, and ^{159}Dy. The observed resolution (FWHM), determined with these K x-ray standards was equivalent to 5.5 nuclear charge units for the NaI detector and 2.0 for the proportional detector.

The preamplified signals from the x-ray and fission-fragment detectors were fed to the amplifiers of a three-

parameter recording system (Fig. 1). Gain stability for all three channels was monitored continuously over the course of each experiment. The maximum gain drift was $\pm 0.3\%$ for the NaI channel (unstabilized) and $\pm 0.1\%$ for the stabilized proportional-counter channel. The fission detectors suffered an unavoidable pulse-height decrease of $\sim 0.6\%$ during each experiment owing to damage by the fragments. (Correction for this effect was made by the computer during data reduction.) A single-channel analyzer selected the pulse-height range of interest for each parameter, and pileup rejectors were used in the fission channels to prevent spectral distortion by the relatively intense alpha radiation from ^{252}Cf. Pulses in triple coincidence were selected by the coincidence circuit, passed through linear gates, digitized in the ADC circuits, stored temporarily in a 512-word 30-bit buffer, and finally stored in groups of 512 words (events) on a 7-track magnetic tape for subsequent computer analysis.

The main bulk of data sorting and reduction was accomplished off-line with a CDC 3600 computer programmed to obtain the initial fission fragment masses and total kinetic-energy distributions, the total kinetic energy as a function of mass, and the coincident K x-ray spectra as a function of mass. Further calculations and data reduction of a less complicated nature, such as mass-resolution corrections, calculation of average masses, and subtraction of prompt γ-ray background and chance coincidence effects, were accomplished with an IBM 1620 computer. The "background" spectrum of pulse heights in the x-ray region (10–50 keV) caused by the higher-energy prompt γ rays was obtained by using a graded filter (0.5 g Cu/cm^2+0.1 g Al/cm^2), opaque to photons of energy $\lesssim 50$ keV.

B. Fragment Mass Distributions

The initial fragment masses (before neutron emission) were computed for each event in the following manner: (a) the final energies of the coincident fragments (after neutron emission) were calculated from the observed pulse heights using the final-fragment-mass-dependent energy calibration described by Schmitt *et al.*[11]; (b) these final energies were corrected for the average number of neutrons emitted as a function of the fragment mass, $\bar{\nu}_A$, using the data of Bowman *et al.*,[12] to yield the kinetic energies of the light and heavy fragments, E_L and E_H, before neutron emission; (c) the initial masses of the fission fragments, A_L and A_H, were then calculated using the following equations:

$$A_L = A_F[E_H/(E_L+E_H)] \text{ and } A_H = A_F - A_L, \quad (1)$$

where A_F is the mass of the fissioning nucleus.

Since the calculations (a) and (b) depend on the initial and final fragment masses, these masses were first approximated. From the initial masses calculated after the first approximation and from the neutron emission data,[12] better estimates of the initial and final masses were obtained. The calculations (a) through (c) were then repeated until the computed initial masses for each event converged to within 0.1 amu.

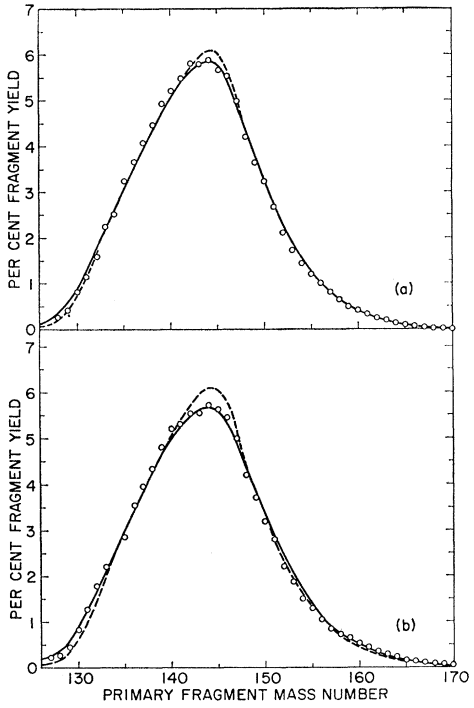

FIG. 2. Binary mass distributions for spontaneous fission of ^{252}Cf obtained from double-fragment kinetic energy measurements. Open circles represent experimental data from this work. Dashed curves show, for comparison, the mass distribution obtained directly by time-of-flight techniques (Ref. 13) with an experimental mass resolution FWHM=2.1 amu. (a) Mass distribution obtained during proportional counter experiments. Solid curve shows the mass distribution calculated by dispersing the time-of-flight mass distribution (corrected for experimental resolution) using a Gaussian dispersing function with σ_T^2 given by Eq. (2) and B=0; average FWHM=4.2 amu. (b) Mass distribution obtained during NaI experiments. Solid curve same as in (a) except $B=2.5$; average FWHM=5.6 amu.

The mass resolution for each experiment was determined by comparing the computed binary mass distribution with that determined by Whetstone[13] using time-of-flight techniques (dashed curves in Fig. 2). The mass resolution in Ref. 13 is relatively small and well known (FWHM=2.1 amu). The mass distribution from Ref. 13 was first corrected for the quoted mass resolution and then dispersed with a Gaussian function having a total variance, σ_T^2, given by Eq. (2).

$$\sigma_T^2(A_{L,H}) = \frac{4\bar{\nu}A_L A_H M_N \bar{E}_N}{3A_F \bar{E}_T} + \tfrac{1}{4}\sigma^2(\bar{\nu}) + \frac{0.41}{\bar{E}_T^2}[A_L^2 + A_H^2] + B. \quad (2)$$

[11] H. W. Schmitt, W. E. Kiker, and C. W. Williams, Phys. Rev. **137**, B837 (1965).

[12] H. R. Bowman, J. C. D. Milton, S. G. Thompson, and W. Swiatecki, Phys. Rev. **129**, 2133 (1963).

[13] S. L. Whetstone, Phys. Rev. **131**, 1232 (1963).

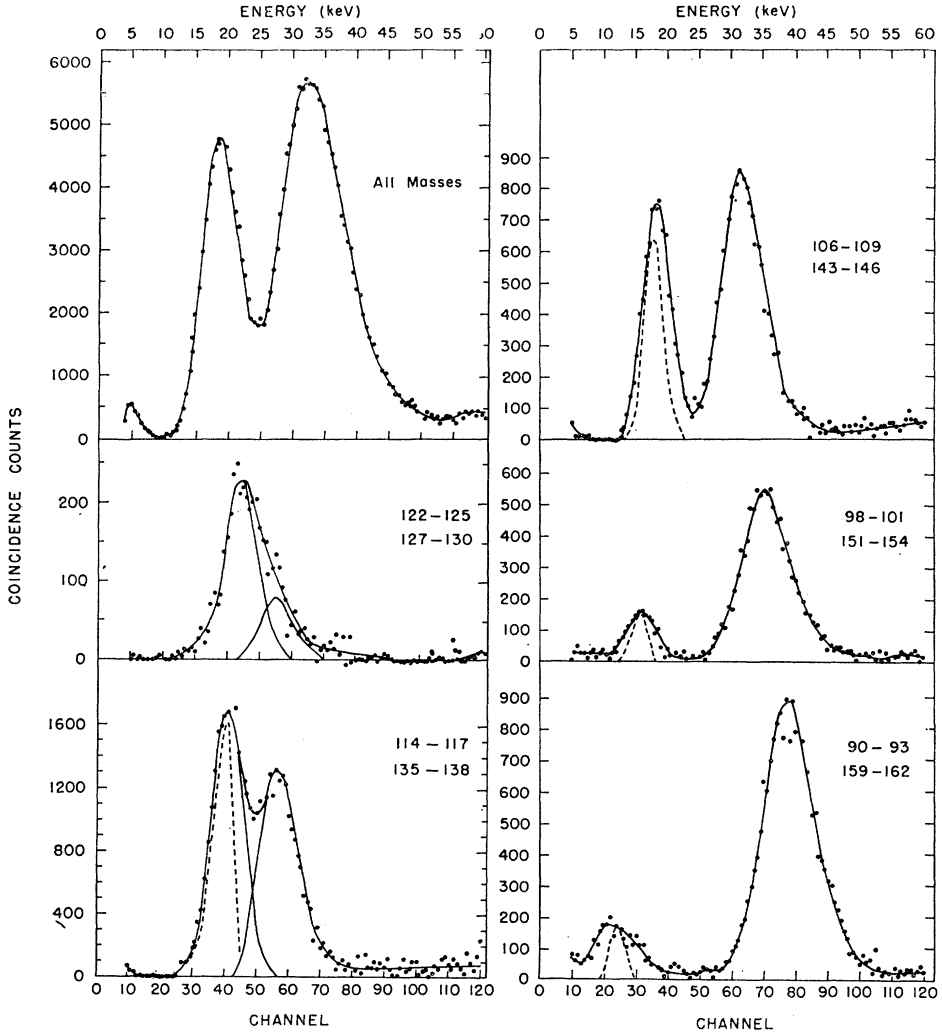

FIG. 3. Energy spectra of K x rays emitted by ^{252}Cf fission fragments for various complementary mass intervals. Spectra obtained with a NaI detector and a gas-flow proportional detector are shown as continuous and broken curves, respectively.

Here $\bar{\nu}$ represents the average total number of neutrons emitted from A_L and A_H; $\bar{M}_N$ and $\bar{E}_N$ are the mass and average center-of-mass energy of the neutrons; $\bar{E}_T$ is the average total fragment kinetic energy; and $\sigma^2(\bar{\nu})$ is the variance about the average number of emitted neutrons. The dominant first two terms of Eq. (2) approximate the broadening for a calculated mass due to varying directions, energies, and numbers of emitted neutrons[14]; the third small term is due to an apparent intrinsic energy resolution (FWHM = 1.5 MeV) for heavy-ion energies measured with solid-state detectors[11]; and the last term B is an empirically adjustable parameter to take into account any unexpected instrumental mass broadening. The solid curve of Fig. 2(a) shows the result of this computation, for $B=0$, compared with the experimentally determined binary mass distribution (open circles) obtained during the experiments in which the proportional x-ray detector was used. The mass resolution established in this manner corresponds to an average FWHM = 4.2 amu. The binary mass distribution obtained during experiments with the NaI x-ray detector exhibited a broader mass resolution due to poorer quality fission-fragment detectors. By empirical adjustment of B a mass resolution with an average FWHM = 5.6 amu was determined for these experiments. With this resolution, the mass distribution calculated using Whetstone's unfolded mass distribution is shown as a solid curve in Fig. 2(b) to be compared with the experimental mass distribution (open circles). Within the experimental errors of both measurements, the agreement of our calculated binary mass distributions with the dispersed time-of-flight mass distribution is very good and lends confidence to the mass resolution used in this work for the determination of the average fragment mass for a given mass interval.

C. Energy and Yield of K X Rays as a Function of Mass

The K x-ray pulse-height data for each coincident event were sorted by the computer according to the

[14] J. Terrell, Phys. Rev. **127**, 880 (1962).

TABLE I. Values of K x-ray yield per fragment (X/f) and most probable nuclear charge (Z_P) as a function of fragment mass.

Selected mass interval	Average initial mass	Average final mass	Z_P	X/f (observed)	X/f (corrected)
86–89[a]	88.8±1.0[a]	87.7[a]	35.1±0.6[a]	0.04 ±0.02[a]	0.04 ±0.02[a]
90–93[a]	92.4±1.0[a]	91.0[a]	36.0±0.5[a]	0.04 ±0.01[a]	0.04 ±0.01[a]
94–97[a]	96.6±0.6[a]	95.2[a]	38.2±0.3[a]	0.04 ±0.01[a]	0.03 ±0.01[a]
98–101[a]	100.8±0.3[a]	99.5[a]	39.8±0.2[a]	0.06 ±0.01[a]	0.06 ±0.01[a]
98–101	101.6±0.3	100.3	39.9±0.2	0.057±0.005	0.053±0.005
102–105[a]	104.4±0.3[a]	102.9[a]	40.9±0.2[a]	0.09 ±0.01[a]	0.10 ±0.01[a]
102–105	105.1±0.3	103.6	41.4±0.2	0.094±0.005	0.11 ±0.01
106–109[a]	107.7±0.3[a]	105.9[a]	42.2±0.2[a]	0.12 ±0.01[a]	0.13 ±0.01[a]
106–109	107.9±0.3	106.1	42.6±0.2	0.115±0.003	0.125±0.006
110–113[a]	111.1±0.3[a]	108.9[a]	43.2±0.2[a]	0.11 ±0.02[a]	0.11 ±0.02[a]
110–113	111.0±0.3	108.8	43.8±0.2	0.123±0.006	0.14 ±0.01
114–117[a]	115.2±0.3[a]	112.3[a]	45.0±0.3[a]	0.10 ±0.02[a]	0.09 ±0.02[a]
114–117	114.7±0.3	111.9	45.2±0.2	0.106±0.005	0.08 ±0.01
118–121[a]	118.4±0.4[a]	114.8[a]		0.12 ±0.03[a]	0.13 ±0.03[a]
118–121	118.2±0.3	114.7	47.1±0.5	0.13 ±0.01	0.15 ±0.01
122–125	120.5±0.6	116.6	47.1±0.5	0.12 ±0.01	0.14 ±0.02
127–130	131.8±1.0	131.1	52.4±1.0	0.05 ±0.01	0.05 ±0.01
131–134	134.9±1.0	133.8	52.7±1.0	0.05 ±0.01	0.05 ±0.01
135–138	138.2±0.5	136.8	53.1±0.2	0.096±0.005	0.12 ±0.01
139–142	141.3±0.3	139.6	54.8±0.2	0.137±0.004	0.15 ±0.01
143–146	144.8±0.3	143.1	55.9±0.2	0.168±0.005	0.16 ±0.01
147–150	148.6±0.3	146.6	57.3±0.2	0.258±0.007	0.29 ±0.01
151–154	152.3±0.3	149.9	59.0±0.2	0.49 ±0.03	0.54 ±0.03
155–158	155.7±0.3	152.9	60.5±0.2	0.84 ±0.04	1.00 ±0.06
159–162	158.9±0.5	155.7	61.6±0.2	0.87 ±0.04	0.95 ±0.06
163–166	162.3±0.8	158.6	63.2±0.3	0.67 ±0.05	0.7 ±0.1
167–170	166 ±2	162.2	64.9±0.5	0.60 ±0.05	0.6 ±0.1

[a] Data for experiments with proportional x-ray detector; all other data with NaI detector.

calculated initial fragment mass distribution into complementary mass intervals of 4 amu over the range $A_L=82$ to 125 and $A_H=127$ to 170. Some typical K x-ray energy spectra for several intervals over this range are shown in Fig. 3 in comparison with the unsorted spectrum for all masses. The plotted points and solid curves represent data obtained with the NaI detector. Typical spectra obtained with the proportional counter are shown (dashed curves with arbitrary ordinate) for four intervals in the light-group mass region. The use of the proportional counter was required for the region below mass 100 where good K x-ray spectra could not be obtained with the NaI scintillator due to serious interference by the escape peak for K x rays ($E>33$ keV) of the heavy group. The argon-methane proportional counter was not useful, however, for K x-ray measurements in the heavy group because of its poor efficiency at higher energies. The spectra in Fig. 3 illustrate clearly the expected trend of average K x-ray energy with mass and also reveal the interesting fact that near symmetry (spectrum at left center) the emission of K x rays by the light fragment is greater than that for the heavy, whereas the reverse is true for very asymmetric mass splits (spectrum at right center).

The determination of the most probable nuclear charge for each mass interval was based on the most probable channel number of each K x-ray spectrum. The most probable channel number was associated with nuclear charge by means of a most probable channel number (determined in an identical manner) versus nuclear charge relationship obtained from the K x-ray standards listed previously (Sec. IIA.). These K x-ray standards extended over the full range of nuclear charge investigated in this work.

The yields of K x rays per fission fragment obtained from the K x-ray energy spectra are listed in Table I as observed (column 5) and corrected for mass resolution (column 6). The corrected yields are plotted in Fig. 4 as a function of the final fragment mass (column 3) corresponding to the selected mass interval (column 1). Kapoor *et al.*[15] also present in the following paper a K x-ray per fragment distribution for ^{252}Cf fission. Although the two experimental distributions are similar, quantitative comparisons are difficult to make because of the grossly different time intervals after fission for K x-ray emission studied in this work (1 nsec) and in their work (50 nsec). The emission of K x rays is seen to be a pronounced function of mass rather analogous to the saw-tooth neutron emission function[12] which reflects the excitation energy of the fragments. Since the K x rays arise predominantly from internal conversion of the prompt γ rays,[8,9] the yield of K x rays per fragment would be expected to depend not only on the excitation energy but also on the nuclear structure of the fragments, i.e., the number, energy, and multipolarity of the prompt γ rays emitted in the deexcitation of each fragment. The observed distribution

[15] S. S. Kapoor, H. R. Bowman, and S. G. Thompson, following paper, Phys. Rev. **140**, B1310 (1965).

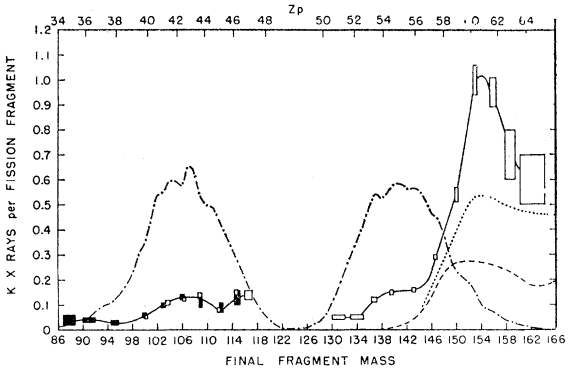

FIG. 4. Yield of K x rays emitted by ^{252}Cf fission fragments within 1 nsec after fission as a function of final fragment mass and Z_P. Size of data symbol represents estimated errors in determinations of yield and mass. □, NaI data; ■, proportional counter data; (·—·) final fragment mass distribution (Ref. 11) (in percent $\times 10^{-1}$); (– – –) calculated K x-ray yields for $E2$ transitions between the first 2+ excited states to 0+ ground states of even-even nuclei; (···) calculated K x-ray yields for cascades of $E2$ transitions through the ground-state rotational bands of even-even nuclei starting from the 8+ state. If all types of nuclei (even-even, odd-odd, etc.) are formed with equal probability in fission, these calculated yields for even-even nuclei should be multiplied by $\frac{1}{4}$ in order to be compared with the experimental yields per fission fragment.

of K x rays may then be interpreted qualitatively in terms of fragment excitation energy and nuclear structure in the following way. In the lighter fragments of the light-mass ($A<98$) and heavy-mass ($A<135$) groups near the closed shells ($N=50$) and ($Z=50$, $N=82$) where excitation energies and level densities are lower, fewer γ rays[16] (possibly of higher average energy) should be emitted resulting in a lower yield of K x rays. Conversely, in the heavier fragments of the two mass groups where excitation energies and level densities are higher, one might expect enhanced emission of γ rays[16] (possibly of lower average energy) and hence an increased yield of K x rays. In addition, the sharp increase at about mass 145 ($N\approx 89$) coincides with and most probably is due to the onset of the region of deformed nuclei characterized by rotational states and an abundance of low-energy (highly converted) $E2$ transitions. A conclusive illustration of this point is the yield of K x rays from internal conversion of the $E2$ transitions between the first 2+ excited states and the 0+ ground states of even-even nuclei shown as a dashed curve in Fig. 4. These $E2$ transitions are used qualitatively here as a measure of the fragment deformation. In going from essentially spherical to deformed nuclei, the energies of these $E2$ transitions decrease sharply, and there is a corresponding rapid increase in K internal conversion and hence in the yield of K x rays. For this calculation the energy of the first 2+ excited state of each most probable even-even fragment was determined by extrapolation of known data,[17] and the K, L, and M conversion coefficients computed by Rose[18] were used. Clearly the agreement of the calculated and experimental mass dependence of the rapid increase in K x-ray yield supports the conclusion that this increase is due to the onset of the region of deformed nuclei.

Fission fragments are known to possess relatively high angular momenta. From the fission-fragment gamma-ray angular distribution studies of Hoffman[19] on thermal-neutron-induced fission of ^{235}U, the average angular momentum of the fragments was determined to be $(7\pm 2)\hbar$. It is therefore not unreasonable to expect in the gamma-ray de-excitation of the fragments that rotational states up to nearly comparable angular momenta would be populated. The dotted curve of Fig. 4 illustrates the upper limiting condition of the K x-ray yield for gamma-ray cascades originating from the 8+ rotational states and proceeding to the 0+ ground states of even-even fragments. In this calculation the energies of the rotational states were obtained by using the previously extrapolated energies of the 2+ excited states and the rotational energy equation, $E_I=(\hbar^2/2\mathcal{I})\times I(I+1)$. If all types of fragments (even-even, odd-odd, etc.) are formed with equal probability in fission, then the calculated dotted curve of Fig. 4 should be reduced by a factor of 4 to obtain the contribution of this type of de-excitation in only even-even nuclei to the gross K x-ray per fragment distribution. Clearly this type of de-excitation in a single rotational band of even-even nuclei cannot account for the magnitude of the observed K x-ray yield. However, similar rotational cascades occurring in the odd-mass fragments and odd-odd fragments may contribute much larger yields of K x rays. For approximately the same initial high rotational angular momentum, the rotational cascade transitions in odd-mass nuclei will be of lower average energy (yielding more K x rays). Furthermore, within the first few MeV of excitation energy more rotational bands (based on different K quantum numbers) exist in odd-mass and odd-odd nuclei than in the even-even nuclei. As an example, for a fragment with $Z=60$ and $A=153$ having a moment of inertia 1.26 times larger than the even-even fragment of mass 152 (an average value calculated from moments of inertia tabulated by Mottelson and Nilsson),[20] 2.6 or 1.4 K x rays per cascade originating from the 15/2+ rotational state would be expected if all the transitions were either $M1$ or $E2$, respectively. Therefore, averaging over the K x-ray contributions from even-even, odd-odd, and odd-mass fragments, a K x ray per fragment yield of ~ 1 at mass ~ 154 would not be unreasonable in light of the interpretation that the large yield of K x rays in this region comes from internal conversion of low-energy rotational

[16] S. A. E. Johansson, Nucl. Phys. **60**, 378 (1964).
[17] *Nuclear Data Sheets*, compiled by K. Way *et al.* (Printing and Publishing Office, National Academy of Sciences–National Research Council, Washington 25, D. C., 1965).
[18] M. E. Rose, *Internal Conversion Coefficients* (North-Holland Publishing Company, Amsterdam, 1958).
[19] M. M. Hoffman, Phys. Rev. **133**, B714 (1963).
[20] B. R. Mottelson and S. G. Nilsson, Kgl. Danske Videnskab. Selskab, Mat. Fyz. Skrifter **1**, No. 8 (1959).

cascade transitions in one or more rotational bands per fragment.

A plausible explanation for the decrease in the yield of K x rays per fragment beyond mass 155 has been suggested by Vandenbosch.[21] A considerable fraction of the K x rays come from conversion in low-energy transitions, some of which have energies near the K-electron binding energy. If the energies of these transitions are approximately constant, or decreasing with increasing fragment mass, the percentage of K conversion per transition will decrease with increasing atomic number and K-electron binding energy. This effect is illustrated in the dashed curve of Fig. 4 for the yield of K x rays from the 2+ to 0+ $E2$ transition. The extrapolated energies of the first 2+ excited states for atomic numbers from 60 to 64 are approximately constant (~70 keV), and the decrease in the calculated yield of K x rays over this region is primarily due to the increasing K-electron binding energies. This effect is clearly illustrated in Fig. 5a for $E2$ transitions; it is seen from Fig. 5b that this effect is much less important for $M1$ transitions. Since the even-even nuclei are expected to be responsible for only a fraction of the K x-ray yield at mass ~154, then in order to account for the magnitude of the decrease in K x ray per fragment yield using this interpretation, a sizable fraction of the transitions giving rise to K x rays in odd-mass and odd-odd fragments must be slightly above the K-electron binding energy and be predominantly of $E2$ multipolarity. More detailed calculations for the odd-mass and odd-odd nuclei cannot be performed at this time, because the results of such calculations are very dependent on poorly known parameters such as the populations of the various rotational states and also the ground-state spins.

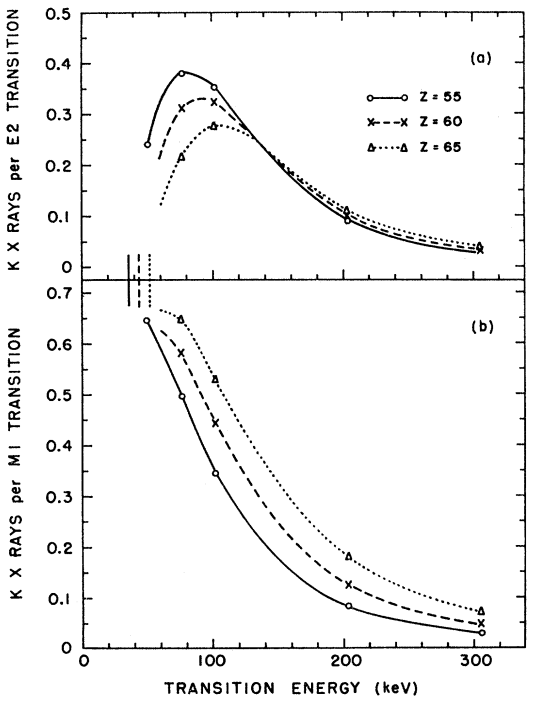

FIG. 5. Yield of K x rays per transition as a function of transition energy and nuclear charge for (a) $E2$ transitions and (b) $M1$ transitions. The vertical lines at left center represent the K-electron binding energies.

[21] R. Vandenbosch (private communication).

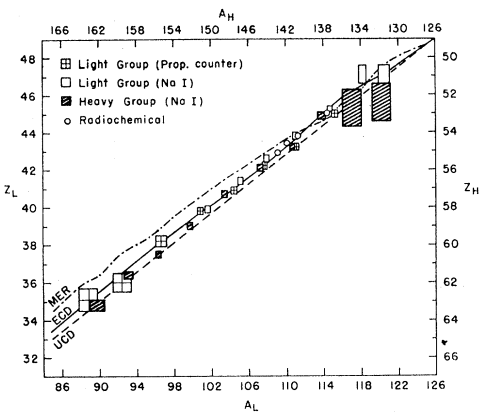

FIG. 6. Most probable nuclear charge as a function of initial fragment mass. Charge and mass of light-group (Z_L,A_L) and heavy-group (Z_H,A_H) fragments are folded around symmetric fission (Z=49 and A=126). Curves for various postulates of charge division are identified as MER (·–·), maximum energy release; ECD (——), equal charge displacement; and UCD (– – –), unchanged charge density.

III. RESULTS AND DISCUSSION

Values for the most probable nuclear charges (Z_P) of the fission fragments, obtained from the observed K x-ray energy spectra (Sec. IIC.), are tabulated in Table I, column 4. Values of the average initial and final fragment masses for each mass interval, corrected for experimental mass resolution (Sec. IIB.) and the observed variation of K x-ray yield with mass (Fig. 4), are listed in Table I (columns 2 and 3). The Z_P values are plotted as a function of initial mass in Fig. 6. Estimated errors in the determination of charge and mass are indicated by the size of the data symbol and are also given in Table I. Also shown in Fig. 6 for comparison with the experimental data are Z_P functions according to various postulates for the most probable charge division in fission. The unchanged charge density (UCD) function is based on the simple assumption that the charge-to-mass ratio of the fragments is constant and equal to that of the fissioning nucleus (Z_F/A_F =0.3889 for ^{252}Cf). The maximum energy release (MER) function represents the charge division corresponding to the maximum release of energy in fission as calculated for ^{252}Cf by Milton.[12] The equal charge displacement (ECD) function is given by the empirical rule[1] that the most probable charges of complementary fragments are equally displaced from the stability line Z_A, i.e., $(Z_A-Z_P)_L=(Z_A-Z_P)_H$. For calculation of the ECD function Z_A values were taken from the analysis

TABLE II. Values of most stable nuclear charge (Z_A) as a function of mass (A).

A	Z_A	Z_A–0.4A	A	Z_A	Z_A–0.4A	A	Z_A	Z_A–0.4A
70	31.13	3.13	104	45.43	3.83	138	56.94	1.74
72	31.93	3.13	106	46.17	3.77	140	58.18	2.18
74	32.73	3.13	108	46.90	3.70	142	59.28	2.48
76	33.51	3.11	110	47.64	3.64	144	60.21	2.61
78	34.30	3.10	112	48.35	3.55	146	61.02	2.62
80	35.00	3.00	114	49.02	3.42	148	61.78	2.58
82	35.74	2.94	116	49.60	3.20	150	62.47	2.47
84	36.53	2.93	118	50.12	2.92	152	63.12	2.32
86	37.41	3.01	120	50.53	2.53	154	63.68	2.08
88	38.37	3.17	122	51.14	2.34	156	64.25	1.85
90	39.33	3.33	124	51.88	2.28	158	64.88	1.68
92	40.27	3.47	126	52.60	2.20	160	65.56	1.56
94	41.22	3.62	128	53.31	2.11	162	66.25	1.45
96	42.15	3.75	130	53.97	1.97	164	66.94	1.34
98	43.06	3.86	132	54.61	1.81	166	67.67	1.27
100	43.90	3.90	134	55.27	1.67	168	68.40	1.20
102	44.68	3.88	136	55.93	1.53	170	69.15	1.15

of beta-decay energies by Dewdney[22] and the table of nuclidic masses by Hillman,[23] both of which are based on the mass values given by König, Mattauch, and Wapstra.[24] The average of the Z_A values from these compilations (which are in good agreement and differ only slightly from those used in Ref. 1) are plotted as $Z_A-0.4A$ at each mass number in Fig. 7. The recommended average Z_A values from the smooth curve of Fig. 7 are listed for convenient use in Table II at even mass numbers from 70 to 170 (from which values at any mass may be interpolated). It is apparent from Fig. 6 that only the ECD function is in reasonable agreement with the experimental data. The radiochemical data for ^{252}Cf fission (open circles) based on fractional chain-yield measurements[3] for ^{136}Cs, ^{139}Xe, ^{140}Xe, and ^{141}Xe are also in good agreement with the data obtained in this work and with the ECD function.

A more sensitive test for fit of the experimental data to the various Z_P functions is provided in Fig. 8 where the function $Z_P-A(Z_F/A_F)$, representing the difference of the most probable charge Z_P from that given by the charge density of the fissioning nucleus (UCD), is

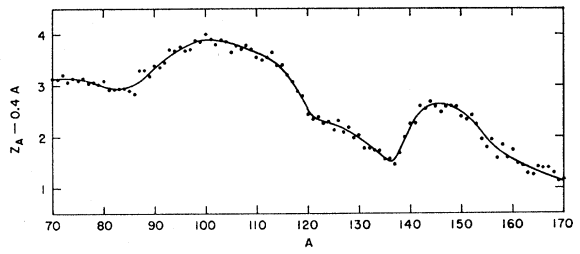

FIG. 7. Smooth Z_A function (plotted as Z_A–0.4A versus A) obtained from Z_A values given by Dewdney (Ref. 22) and Hillman (Ref. 23). The data points represent the average of the Z_A values from the two references at each mass number.

[22] J. W. Dewdney, Nucl. Phys. **43**, 303 (1963).
[23] M. Hillman, Brookhaven National Laboratory Report BNL-846 T-333, 1964 (unpublished).
[24] L. A. König, J. H. E. Mattauch, and A. H. Wapstra, Nucl. Phys. **31**, 18 (1962).

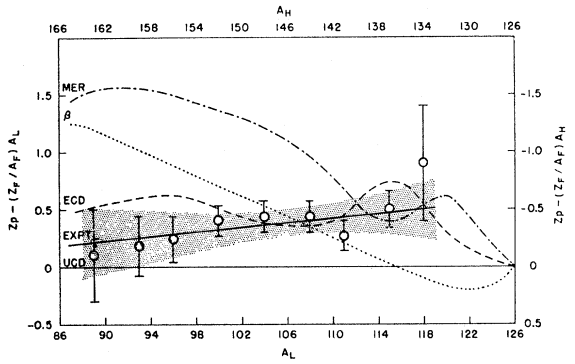

FIG. 8. Difference of the most probable nuclear charge from that given by the charge density of the fissioning nucleus, $Z_P-A\times(Z_F/A_F)$, as a function of initial fragment mass. The functions MER (·–·), ECD (– – –), and UCD (——) are defined in the caption for Fig. 6. The function β (···) is due to Armbruster (Ref. 25) and represents the charge division expected from the postulate of MER between saddle point and scission. The straight line EXPTL is the result of a linear least-squares fit to the Z_P data of Table I over the mass ranges 89–118 and 134–163 (with heavy-group data converted to light-group complements); the shaded area represents the error band (90% confidence level) for the least-squares analysis. The data points are averages of the data in Table I for the various mass splits (over the same range of masses).

plotted against initial fragment mass (light group, A_L and heavy group, A_H). The straight line EXPTL is the result of a weighted linear least-squares fit to the experimental data over the mass ranges 89–118 and 134–163 (with heavy-group data converted to light-group complements). The shaded area represents the error band (90% confidence level) for the least-squares analysis. The data for the nine mass splits (complementary mass intervals) over this range were averaged at each mass split to give the plotted points. The Z_P function β was calculated by Armbruster[25] and represents the charge division expected for ^{252}Cf by the postulate of maximum energy release between saddle point and scission which is in agreement with his measurements[2] of the average β-decay-chain lengths in thermal-neutron-induced fission of ^{235}U. It is clearly evident that among the various Z_P functions only ECD is reasonably consistent with the experimental data. Also using the K x-ray method in a study of ^{252}Cf fission, Kapoor *et al.*[15] have obtained similar results and gave come to the same conclusion.

A few concluding remarks should be made regarding the reliability of the K x-ray method for determination of fragment nuclear charge. Since the K x rays are evidently produced by the process of internal conversion,[8,9] there is the possibility that the process might be selective and give rise to K x rays not representative of the average nuclear charge for a given mass interval. In this case one would expect to find local deviations (well outside of experimental error) in the Z_P values

[25] P. Armbruster, Proceedings of the IAEA Symposium on the Physics and Chemistry of Fission, Salzburg, 1965, paper SM-60/11 (to be published).

from one mass interval to another, and also failure of charge conservation ($Z_L+Z_H=Z_F$) for the complementary Z_P values associated with a given mass split. By reference to Fig. 6 it is seen that these signs of selectivity do not occur, even in the complementary mass regions 92–104 and 148–160 where there is a wide disparity in K x-ray yield (see Fig. 4). The experimental value for Z_F (weighted average of all mass splits) is 98.1 ± 0.1. It is therefore concluded from this work that the K x-ray method gives a reasonably accurate picture of charge division.

In the future, the experimental method described in this work can yield much more information on charge distribution in nuclear fission than already presented here. For example, the nuclear charge dispersion about the most probable charge can be determined when the mass resolution (obtained in double-kinetic energy measurements) is known more accurately by direct measurement, and x-ray detectors of slightly better resolution than those used in this work are available. Also, correlations between the nuclear charges of the fragments and the total kinetic energy release for given mass divisions can be studied. We have analyzed some of our data for such a correlation and have found, for fragments in mass intervals with average masses of 107.9, 144.8, and 155.7, that the average nuclear charges of these fragments remain constant to within an experimental uncertainty of 0.4 Z units on changing the average total kinetic energy release from 170 to 199 MeV.

ACKNOWLEDGMENTS

The authors wish to express their gratitude to Dr. H. C. Griffin for his participation during the early stages of the experimental work and to the Argonne heavy element chemistry group for making available sources of ^{252}Cf. We are also indebted to Dr. R. Vandenbosch and Dr. T. D. Thomas for suggestions and discussions concerning the interpretation of the K x-ray yield distribution. Dr. J. Fiedler kindly provided us with elaborate compilations of the most recent literature Z_A values, and Dr. A. H. Jaffey contributed helpful information concerning the statistical analysis of the experimental data.